34 % yield was reported in the preparation of **2e** from **1e** and *t*BuOCl/HgI_2, see reference [4].
[9] None of the bifunctional derivatives **3** were observed when performing the reaction under photochemical conditions, even using an excess of $PhI(OAc)_2$. For instance, when **1a** was treated with $PhI(OAc)_2$ (2 equiv), I_2 (1.1 equiv), and *t*BuOH (2 equiv) under the influence of light at room temperature, only the formation of **2a** was observed after 8 h, the excess $PhI(OAc)_2$ was recovered.
[10] For recent evidence: a) J. Madsen, C. Viuf, M. Bols, *Chem. Eur. J.* **2000**, *6*, 1140–1146; b) J. L. Courtneidge, J. Lusztyk, D. Pagé, *Tetrahedron Lett.* **1994**, *35*, 1003–1006.
[11] J. Gallos, A. Varvoglis, *J. Chem. Soc. Perkin Trans. 1* **1983**, 1999–2002.
[12] We have observed that **2b** was cleanly converted into **3b** under comparable thermal conditions, thus providing additional evidence for the proposed mechanism.

Mechanism of the Transformation of Silica Precursor Solutions into Si-MFI Zeolite

Svetlana Mintova,* Norman H. Olson, Jürgen Senker, and Thomas Bein*

Dedicated to Professor Jens Weitkamp on the occasion of his 60th birthday

The mechanisms governing the transformation of precursor solutions or gels into zeolitic materials are still not fully understood.[1–5] The scientific challenge is to understand these mechanisms to enhance synthetic control for the design of new zeolite structures, and for the preparation of novel assemblies such as films, monoliths, and functional nanostructures.

The crystal growth of silicalite-1—a microporous polymorph with MFI topology—has received considerable attention because it can serve as model system for a fundamental understanding of the mechanism of zeolite formation.[6–9] The nanoscale organosilicate clusters in the precursor solutions used for the synthesis of nanosized MFI-type zeolite have been observed with techniques such as dynamic light scattering (DLS),[6] nuclear magnetic resonance (NMR),[7, 8] small-angle X-ray scattering (SAXS),[9, 10] and high-resolution transmission electron microscopy (HRTEM).[11–13] It appears that nanoscale species with a size of about 3–4 nm are formed in the precursor solutions before long-range order is established.[14, 15] Additional information about the structure, particle size, and shape of the silicate species in the MFI-precursor solutions containing organic additives was obtained by using NMR spectroscopy[16] and in situ SAXS measurements.[9, 10] These studies suggest that the aggregation of the primary units is an important step in the nucleation process, and that it depends on many factors, such as the alkalinity of the precursor solution, the type of silica source, and aging time. However, structural information regarding the initial framework species assembled from molecular precursors is still very limited.

In previous studies we have investigated the nucleation and growth processes of zeolites A (LTA) and Y (FAU) (using the tetramethylammonium (TMA) ion) by HRTEM.[11] It was observed that the crystalline structures nucleate in amorphous gel aggregates existing in the colloidal aqueous solutions, and that these gel aggregates are completely converted into crystalline products after extended reaction times.

Herein, we examine the formation of the colloidal precursor solution and the crystal growth of Si-MFI by in situ DLS combined with ^{29}Si solid-state NMR spectroscopy, HRTEM, and other techniques.

A clear precursor solution, prepared for the synthesis of Si-MFI zeolite, was aged at room temperature on an orbital shaker for 24 h (A24h) to 30 days (A30d). Samples were heated to 90 °C and then examined by in situ DLS measurements. A major advantage of the in situ study is the elimination of invasive procedures that may modify the crystallization process of the Si-MFI zeolite. Figure 1 shows

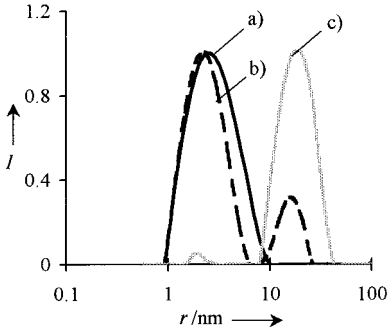

Figure 1. DLS data of TPA-silica precursor solutions: a) aged for 24 h (A24h) at room temperature, and after heating for b) 4 min (A24hH4m) and c) 6 h (A24hH6) at 90 °C. The distribution function analysis (DFA) is displayed as scattering intensity per unweighted particle size classes (I = scattering intensity).

the particle size (r) distribution of the precursor solution aged for 24 h (A24h), and for samples heated to 90 °C for 4 min (A24hH4m) and 6 h (A24hH6). Prior to heating, the presence of sub-colloidal particles with sizes in the range of about 1–10 nm is observed in the A24h sample. These particles are shown to be amorphous by X-ray diffraction. After hydrothermal treatment of solution A24h for only 4 min (Figure 1b), an increase of the scattering intensity is observed, due to the presence of a second generation of particles with mean radius of about 15 nm (sample A24hH4m; Figure 1b). The two particle populations present in these samples are quite diverse, the first having a mean radius of about 2.3 nm and the second having a radius of about 15 nm. By increasing the heating time from 4 min to 6 h (sample A24hH6; Figure 1c), the peak indicative for the presence of sub-colloidal

[*] Dr. S. Mintova, Prof. T. Bein, Dr. J. Senker
Department of Chemistry
University of Munich
Butenandtstrasse 5–11, 81377 Munich (Germany)
Fax: (+49) 89-2180-7622
E-mail: svetlana.mintova@cup.uni-muenchen.de
tbein@cup.uni-muenchen.de
Dr. N. H. Olson
Department of Biology
Purdue University
West Lafayette, IN 47907 (USA)

  1433-7851/02/4114-2558 $ 20.00+.50/0

particles (~2.3 nm) is diminished, whereas the peak representing the new generation of particles (~15 nm) becomes more pronounced. The solid products extracted by high-speed centrifugation from the samples A24h and A24hH4m were shown by X-ray analysis to be entirely amorphous, while sample A24hH6 displays Bragg reflections corresponding to the MFI-type structure.[17] The XRD pattern of sample A24h is similar to that depicted in Figure 3a.

After aging the TPA-silica precursor solution for 30 days at room temperature (sample A30d), particles with a radius of between 1 and 15 nm are formed (Figure 2a). The solution remained clear over this extended time period. From the particle size distribution data of this sample, we can conclude that the primary sub-colloidal units are consumed during the long aging period, and that a new particle population is formed. The distribution depicted in Figure 2a shows that upon aging for 30 days, the precursor species rearrange into two distinct particulate forms, with mean radii of about 1 nm and 10 nm, respectively. These particles exhibit X-ray scattering, suggesting the onset of crystalline order of the MFI structure (Figure 3a). After hydrothermal treatment of the samples for 2, 3, and 4 h, the particle size distribution curves show the disappearance of the sub-colloidal fraction (~1 nm) in favor of the formation of larger particles with radii between 10 and 60 nm (Figure 2b, c, d). The appearance of diffraction lines suggests the emergence of crystalline MFI-type zeolite in sample A30dH2, (Figure 3b), with a fully crystalline sample obtained after hydrothermal treatment for 3 h (A30dH3) (Figure 3c).

Analysis by HRTEM supports the results of the X-ray analysis, as formation of crystalline Si-MFI is clearly observed in sample A30d (Figure 4a). This HRTEM image reveals, for the first time, the presence of solid objects with a mean radius in the range of 2–10 nm having crystalline fringes corresponding to the MFI structure. Further evidence of the significant crystallinity of the nanosized particles in sample A30d was obtained from IR spectroscopy. Freeze-dried samples of A30d and A30dH3, prepared in KBr pellets, yielded distinct absorptions at 459 and 557 cm^{-1} for A30dH3, while A30d shows two bands shifted to higher frequencies, at 462 and 580 cm^{-1}. The

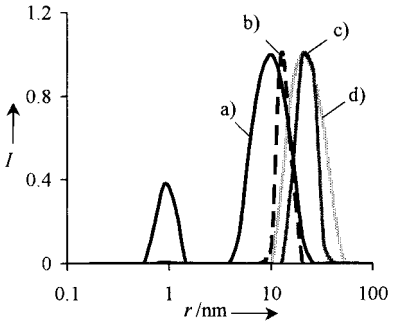

Figure 2. DLS data of TPA-silica precursor solutions: a) aged for 30 days (A30d) at RT, and after heating for b) 2 h (A30dH2), c) 3 h (A30dH3), and d) 4 h (A30dH4) at 90 °C. The DFA is displayed as scattering intensity per unweighted particle size classes.

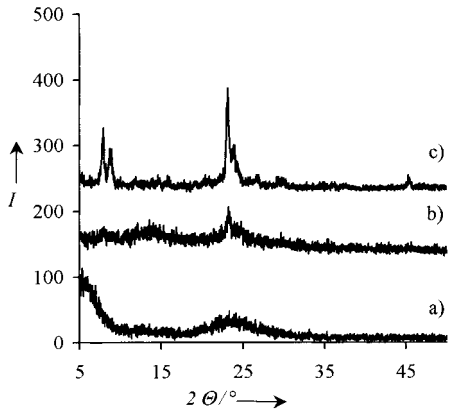

Figure 3. Powder diffraction patterns of a) a precursor solution aged for 30 days (A30d) at room temperature, and after hydrothermal treatment at 90 °C for b) 2 h (A30dH2) and c) 3 h (A30dH3).

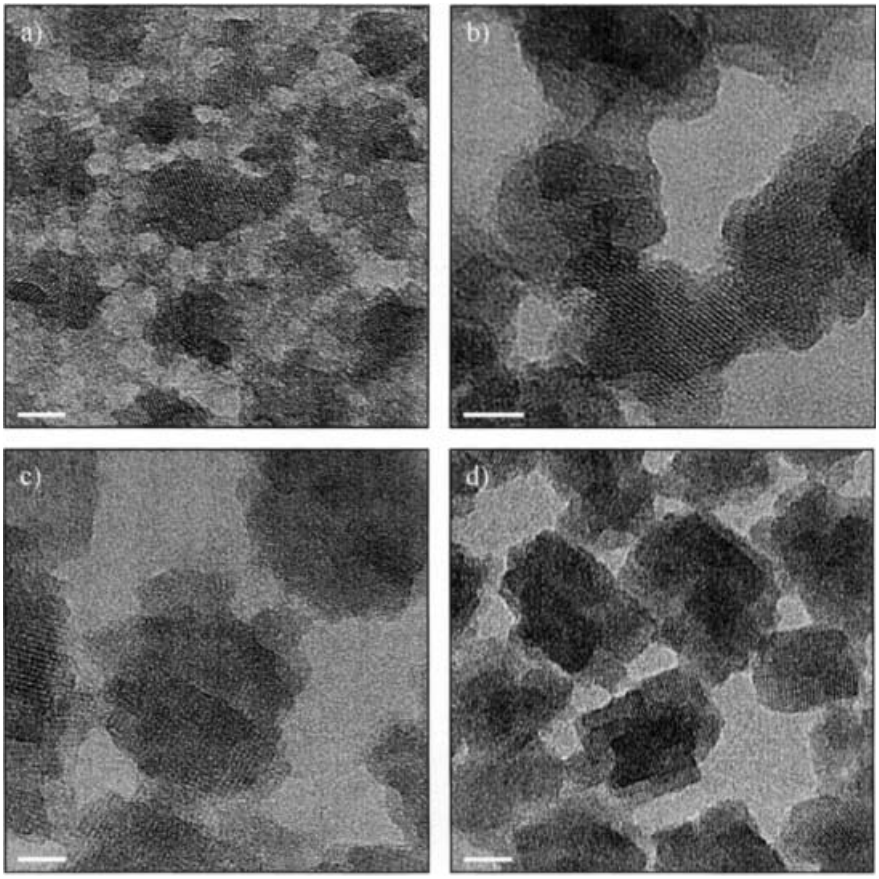

Figure 4. HRTEM images of nanosized particles extracted from a) a TPA–silica precursor solution aged for 30 days (A30d) at room temperature, and after heating for b) 2 h (A30dH2), c) 3 h (A30dH3), and d) 4 h (A30dH4) at 90 °C. Scale bar = 10 nm. (See Experimental Section for details).

  1433-7851/02/4114-2559 $ 20.00+.50/0

frequency shift can be ascribed to the small size of silicate particles containing double 5-rings, while the different ratios between the two bands ($\sim 560/\sim 460\ cm^{-1}$) suggest a lower degree of crystallinity in the A30d sample than in the hydrothermally treated A30dH3 sample.[15] These data confirm that the MFI topology can be formed by aging at room temperature. Notably, the particles are very stable during the sample purification process, which includes one-step centrifugation and ultrasonic redispersion in doubly distilled water.

A complementary ^{29}Si solid-state NMR investigation was performed with the solution A30d and freeze-dried particles of sample A30dH3. Sharp ^{29}Si NMR signals are observed between $\delta = -71.2$ and -98 ppm in sample A30d; these are attributed to Q^0, Q^1, Q^2, and Q^3 units of small silicate species in the liquid phase (Figure 5a). In addition, two broad signals

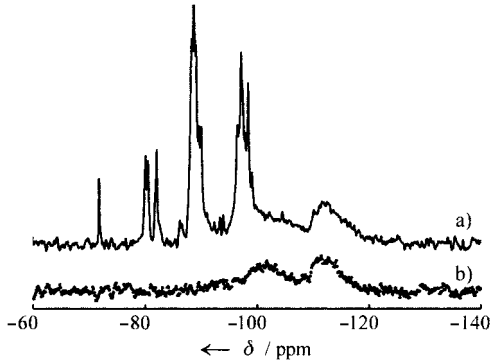

Figure 5. ^{29}Si NMR spectra of a) the as-prepared TPA–silica precursor solution aged for 30 days (A30d) at room temperature and b) the freeze-dried MFI crystalline sample collected from the solution heated at 90 °C for 3 h (A30dH3).

at $\delta = -101.5$ and -112.2 ppm are also observed, indicating the presence of species with mainly Q^3 and Q^4 sites, which correspond to larger condensed polysilicate units in the solid nanoparticles (Figure 5a). The difference in the width of the signals measured for this sample is attributed to the presence of Q^0, Q^1, Q^2, and Q^3 silicate species mainly in the liquid phase, and Q^3 and Q^4 units in the solid phase. In the freeze-dried crystalline MFI sample A30dH3 (Figure 5b), two broad resonance signals are detected with chemical shifts of $\delta = -101.5$ and -112.2 ppm, respectively. The intensity of the two resonance signals, assigned to Q^3 and Q^4 units, is similar. This is probably due to a high concentration of Q^3 silicon existing at the external surface of the nanoparticles, and at internal defects. Since the position and the intensity of the two signals at $\delta = -101.5$ and -112.2 ppm in the liquid and solid samples are similar it is suggested that they are due to the presence of crystalline Si-MFI type nanoparticles in both cases.

During hydrothermal treatment of sample A30d, the crystalline particles grow until the small sub-colloidal particles (~ 1 nm) are completely consumed. The DLS data provide information on the consumption of the nanometer-scale precursor crystalline particles, and the formation of the larger MFI crystals, which display mono-modal particle size distribution (Figure 2). The size distribution measured for sample A30dH3 (3 h HT treatment) is sharper than that for sample A30dH4 (4 h), which is probably due to a more homogeneous distribution of round-shaped colloidal crystals in the former. TEM images of the extracted particles from these samples are shown in Figure 4b, c, and d. The particles in all three samples are single crystals with the expected lattice fringes of MFI-type zeolite. No intergrowth of different lattice orientations is observed, indicating that each crystal was generated from one single-crystalline nanoparticle existing in the aged solution. The Si-MFI crystals obtained from samples A30dH2 and A30dH3 are cauliflower-shaped, while the individual particles in sample A30dH4 have the platelike coffin morphology typical for MFI-type crystals. The formation of crystalline MFI zeolite is more rapid from the solution aged for 30 days (about 3 h) than that obtained after aging for only 24 h(about 6 h). Very effective crystal growth was achieved in the aged precursor solution, where the nutrient pool consists of the sub-colloidal MFI particles formed at room temperature, which resembles Ostwald ripening during crystal growth processes.

In conclusion, we have shown how DLS, HRTEM, and other data provide information about the formation and consumption of particles in reactive organosilica solutions leading to nanoscale crystalline Si-MFI particles. Most strikingly, sub-colloidal precursor particles crystallize within 1 to 30 days at room temperature to form the MFI topology. Additional heating leads to the formation of a second larger crystal-size population at the expense of the sub-colloidal crystals. These findings strongly suggest that the aging step in zeolite synthesis leads to the formation of nanoscale crystalline particles, or domains of the desired zeolite phase. This provides a clear understanding of the paramount importance of such low-temperature pre-treatment steps in zeolite synthesis.

Experimental Section

Nanosized Si-MFI crystals were prepared from clear solutions with a molar composition: 9 TPAOH:25 SiO_2:530 H_2O:100 EtOH. Tetraethoxysilane (TEOS, 98%; Aldrich), tetrapropylammonium hydroxide (TPAOH; Aldrich) and doubly distilled water were used as starting materials. The precursor solution was aged on an orbital shaker (180 rpm) at room temperature for between 24 h and 30 days. Further crystallization was carried out in a quartz cuvette mounted in the DLS instrument with an internal heater set to 90 °C for up to 6 h. All samples with different times of aging and crystallization are specified in Table 1.

In situ DLS was used (ALV-NIBS/HPPS) to investigate the polycondensation process of TEOS in a concentrated aqueous solution of TPAOH at room temperature, and upon hydrothermal treatment at 90 °C. The back scattering geometry (scattering angle 173°, HeNe laser with 3 mW output power at 632.8 nm wavelength) permits measurements at high sample

Table 1. Conditions for the preparation of Si-MFI zeolite.

Sample[a]	Aging time	Crystallization time
A24h	24 h	–
A24hH4m	24 h	4 min
A24hH6	24 h	6 h
A30d	30 days	–
A30dH2	30 days	2 h
A30dH3	30 days	3 h
A30dH4	30 days	4 h

[a] Abbreviations: A = aged sample; H = hydrothermally treated sample.

  1433-7851/02/4114-2560 $ 20.00+.50/0

concentration, because a complete penetration of the incident light through the sample was not required. The distribution function analysis (DFA) data were used to investigate multi-modal particle size distributions in the liquid samples. HRTEM images were recorded by using a Philips CM 200 FEG TEM operated at 200 kV. The ^{29}Si MAS experiments were carried out with 4 mm ZrO_2 rotors in a commercial double resonance probe using a DSX advance impulse spectrometer (Bruker DSX Avance 500) working at a resonance frequency of 99.369 MHz. The samples were examined by using a single-pulse acquisition. The 90° pulse length and the recycle delay were set to 3.0 μs and 40 s. The XRD measurements were performed on a Scintag XDS 2000 diffractometer using $Cu_{K\alpha}$ radiation. IR spectra were recorded from KBr pellets on a Bruker Equinox 55 spectrometer. Prior to the XRD and IR measurements, nanosized crystals were separated from the mother liquor by one-step centrifugation at 20000 rpm for 1 h, and redispersed in an ultrasonic bath in doubly distilled water for 2 h prior to further investigations. Solid products were obtained by freeze-drying of the centrifuged samples.

Received: January 24, 2002 [Z18579]

[1] C. S. Cundy, M. S. Henty, R. J. Plaisted, *Zeolites* **1995**, *15*, 400.
[2] P-P. E. A. de Moor, T. P. M. Beelen, B. U. Komanschek, R. A. van - Santen, *Micropor. Mesopor. Mater.* **1998**, *21*, 263.
[3] S. L. Burkett, M. E. Davis, *Chem. Mater.* **1995**, *7*, 920.
[4] M. Tsapatsis, M. Lovallo, M. E. Davis, *Micropor. Mater.* **1996**, *5*, 381.
[5] M. W. Anderson, J. R. Agger, J. T. Thornton, N. Forsyth, *Angew. Chem.* **1996**, *108*, 1301; *Angew. Chem. Int. Ed. Engl.* **1996**, *35*, 1210.
[6] a) A. E. Persson, B. J. Schoeman, J. Sterte, J.- E. Otterstedt, *Zeolites* **1994**, *14*, 557; b) B. J. Schoeman, *Zeolites* **1997**, *18*, 97; c) B. J. Schoeman, *Micropor. Mesopor. Mater.* **1998**, *22*, 9; d) T. A. M. Twomey, M. Mackay, H. P. C. E. Kuipers, R. W. Thompson, *Zeolites* **1994**, *14*, 162.
[7] C. E. A. Kirschhock, R. Ravishankar, F. Verspeurt, P. J. Grobet, P. A. Jacobs, J. A. Martens, *J. Phys. Chem.* **1999**, *103*, 4965.
[8] S. L. Burkett, M. E. Davis, *J. Phys. Chem.* **1994**, *98*, 4647.
[9] a) P-P. E. A. de Moor, T. P. M. Beelen, R. A. van Santen, *J. Phys. Chem.* **1999**, *103*, 1639; b) P-P. E. A. de Moor, T. P. M. Beelen, R. A. van Santen, L. W. Beck, M. E. Davis, *J. Phys. Chem.* **2000**, *104*, 7600.
[10] a) R. I. Walton, F. Millange, D. O'Hare, A. T. Davies, G. Sanker, C. R. A. Catlow, *J. Phys. Chem.* **2001**, *105*, 83; b) R. I. Walton, D. O'Hare, *J. Phys. Chem.* **2001**, *105*, 91.
[11] a) S. Mintova, N. Olson, V. Valtchev, T. Bein, *Science* **1999**, *283*, 958; b) S. Mintova, N. Olson, T. Bein, *Angew. Chem.* **1999**, *111*, 3400; *Angew. Chem. Int. Ed.* **1999**, *38*, 3201.
[12] O. Regev, Y. Cohen, E. Kehat, Y. Talmon, *Zeolites* **1994**, *14*, 314 – 319.
[13] O. Terasaki, *Molecular Sieves: Science and Technology*, *Vol. 2* (Eds.: H. G. Karge,J. Waitkamp), Springer, Berlin, **1999**, p. 71.
[14] B. J. Schoeman, *Zeolites* **1997**, *18*, 97.
[15] a) R. Ravishankar, C. E. A. Kirschhock, B. J. Schoeman, P.Vanoppen, P. J. Grobet, S. Storck, W. F. Maier, J. A. Martens, F. C. De Schryver, P. A. Jacobs, *J. Phys. Chem. B* **1998**, *102*, 2633; b) R. Ravishankar, C. E. A. Kirschhock, P.-P. Knops-Gerrits, E. J. P. Feijen, P. J. Grobet, P.Vanoppen, F. C. De Schryver, G. Miehe, H. Fuess, B. J. Schoeman, P. A. Jacobs, J. A. Martens, *J. Phys. Chem. B* **1999**, *103*, 4960; c) C. E. A. Kirschhock, R. Ravishankar, L. Van Looveren, P. A. Jacobs, J. A. Martens, *J. Phys. Chem. B* **1999**, *103*, 4972; d) C. E. A. Kirschhock, R. Ravishankar, P. A. Jacobs, J. A. Martens, *J. Phys. Chem. B* **1999**, *103*, 11021; e) C. E. A. Kirschhock, V. Buschmann, S. Kremer, R. Ravishankar, C. J. Y. Houssin, B. L. Mojet, R. A. van Santen, P. J. Grobet, P. A. Jacobs, J. A. Martens, *Angew. Chem.* **2001**, *113*, 2707; *Angew. Chem. Int. Ed.* **2001**, *40*, 2637.
[16] a) S. D. Kinrade, C. T. G. Knight, D. L. Pole, R. T. Syvitski, *Inorg. Chem.* **1998**, *37*, 4272; b) S. D. Kinrade, C. T. G. Knight, D. L. Pole, R. T. Syvitski, *Inorg. Chem.* **1998**, *37*, 4278.
[17] M. M. J. Treasy and J. B. Higgins, *Collection of Simulated XRD Powder Patterns of Zeolites*, 4th rev. ed., Elsevier, Dordrecht, **2001**, p. 234.

Synthesis, Separation, and Characterization of the Topoisomers of Fused Bicyclic Subphthalocyanine Dimers**

Christian G. Claessens and Tomás Torres*

Subphthalocyanines (SubPcs, **1**)—lower homologues of phthalocyanines—are nonplanar cone-shaped aromatic macrocycles comprising three N-fused diiminoisoindoline units around a boron atom core.[1] The 14 π-electron system

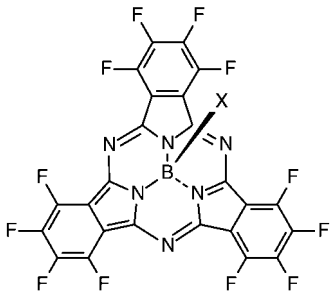

1a X = Cl
1b X = OPh

characteristic of these compounds confers interesting optical properties that have been exploited in the fields of dyes, nonlinear optics, and photonic devices.[1] Moreover, these properties may be fine-tuned since the axial (X) and peripheral positions in SubPcs (see **1**) can be easily functionalized or derivatized.[1] On the other hand, the intrinsic chirality of subphthalocyanines with C_3 or C_1 symmetries represents[2] also a promising feature that enhances their potential as building blocks for the construction of complex molecules.[1]

One focus of our current efforts is the stepwise synthesis of extended π surfaces.[3] Thus, we have recently described the preparation of heterobinuclear azaporphyrinic systems[4a] as well as multinuclear annulene – phthalocyanines.[4b] In this regard, although fused binuclear phthalocyanine dimers are well-known,[5] only one example of a fused subphthalocyanine dimer analogue, whose characterization data (^1H NMR and UV/Vis spectroscopy) do not agree with any of the characteristic features described herein, has been claimed.[6]

[*] Prof. T. Torres, Dr. C. G. Claessens
Departamento de Química Orgánica
Facultad de Ciencias
Universidad Autónoma de Madrid
Cantoblanco, 28049 Madrid (Spain)
Fax: (+34) 91-397-3966
E-mail: tomas.torres@uam.es

[**] This work was supported by the CICYT (Spain; research project MAT-99-0180) and the European Community (contract HPRN-CT-2000-00020). C.G.C. thanks the CICYT for a "Ramon y Cajal" contract. We thank César J. Pastor Montero from the Servicio Interdepartamental de Investigación de la Universidad Autónoma de Madrid for the X-ray structure elucidation. Editorial Note: See also following communication in this issue: T. Fukuda, J. R. Stork, R. J. Potucek, M. M. Olmstead, B. C. Noll, N. Kobayashi, W. S. Durfee, *Angew. Chem.* **2002**, *114*, 2677; *Angew. Chem. Int. Ed.* **2002**, *41*, 2565.

Supporting information for this article is available on the WWW under http://www.angewandte.org or from the author.

  1433-7851/02/4114-2561 $ 20.00+.50/0